Assessment of ADCIRC's wetting and drying algorithm

J.C. Dietrich[a], R.L. Kolar[a], and R.A. Luettich[b]

[a]School of Civil Engineering and Environmental Science, University of Oklahoma, Norman OK, 73019, cdietrich@ou.edu, kolar@ou.edu

[b]Institute of Marine Sciences, University of North Carolina, Morehead City NC, 28557, rick_luettich@unc.edu

The ADvanced CIRCulation (ADCIRC) model is a finite-element hydrodynamic model based on the generalized wave continuity equation (GWCE). The model assumed fixed land boundaries until a wetting and drying algorithm was implemented by Luettich and Westerink in 1995 [1,2]. The algorithm uses an element-based approach, effectively turning elements on and off based on water depths and a water level gradient. While robust in some simulations, the algorithm can be subject to instabilities in the solution during highly nonlinear events. Thus, a rigorous assessment of the algorithm's stability, accuracy, mass balance properties, and parameter sensitivity under a variety of conditions is needed. Herein, we examine these issues using a one-dimensional implementation of the wetting and drying algorithm for basins with a linear slope; future studies will examine a wider variety of real and idealized basins. We believe the results of this work will benefit similar studies in two- or three-dimensions, for users and developers of both ADCIRC and other finite element models.

1. BACKGROUND

Shallow water equations are used by researchers and engineers to model the hydrodynamic behavior of oceans, coastal areas, estuaries, lakes and impoundments [3]. The finite element solutions of these equations have been improved by two equations: the wave continuity equation (WCE), introduced by Lynch and Gray [4] to suppress the spurious oscillations inherent to the primitive equations without having to dampen the solution either numerically or artificially; and the generalized wave continuity equation (GWCE), introduced by Kinnmark [5] to allow a balance between the primitive and pure wave forms of the shallow water equations by adding a weighted form of the primitive equation to the wave equation and using a weighting parameter G. The finite element model used in this paper, ADCIRC, was developed from the GWCE [6,7].

One area where ADCIRC and other hydrodynamic models may have problems is wetting and drying. Large-scale water behavior is often driven by wind and tides, of which the most notable is the M_2 tide caused by the gravitational effects of the moon. Where the tides meet the shore, the water should move up and down the beach, causing areas to alternate between being wet and dry. Simply ignoring this behavior and treating the

shoreline as a firm boundary, as was done in early versions of ADCIRC, allows the water to build up on boundary nodes as if against a vertical wall, which also affects the manner in which waves reflect. Clearly, this can introduce phase and amplitude errors into near-shore circulation. A more physically-realistic model would turn on and off nodes and elements as the tide advances and recedes, as is done in recent versions of ADCIRC. However, many of its parameters have yet to be rigorously assessed, a problem which forms the basis for this study.

2. METHODS

In this section, we will discuss the implementation of a wetting and drying algorithm in the one-dimensional ADCIRC model. We will also describe our two model problems and the methods in which we assess the errors in our numerical results.

2.1. Wetting and drying algorithm

The one-dimensional ADCIRC wetting and drying algorithm is an approach developed by Luettich and Westerink [1,2] and is based on simplified physics and some empirical rules. The algorithm is located in the middle of the time loop, after the solution of the continuity equation but before the solution of the momentum equation. The algorithm is comprised of three parts.

First, the total water depth at every node is checked against a minimum wetness height, H_{min}. If the total water depth is larger than this minimum value, then the node remains active ("wet") and is included in the rest of the calculations. However, if the total water depth has fallen below this minimum value, then the node is inactive ("dry") and removed from the calculations. Note that a dry node can have a positive water depth that is smaller than H_{min}. To help control oscillations, an input parameter allows the user to control the number of time steps that a node has to remain wet before it can be turned off; for all of the results in this paper, that parameter was set to 5 time steps.

Second, the steady state velocity that would result from a balance between the water level gradient and the bottom friction between a wet and an inactive node is checked against a minimum wetting velocity, U_{min}. The balance is given by:

$$U = \frac{g(\zeta_{i-1} - \zeta_i)}{\tau_i \Delta x_i}, \tag{1}$$

where g is gravity; ζ_{i-1} and ζ_i are the free surface elevations at the adjacent node and the node of interest, respectively; τ_i is the equivalent linear bottom friction coefficient (see Equation 7); and Δx_i is the grid spacing. Note that in many situations, only the free surface elevations will change significantly from time step to time step. In this case, the U_{min} criterion almost becomes a height restriction, where a node wets if the adjacent node's free surface elevation is sufficiently larger than its own. Again, to help control oscillations, another input parameter allows the user to control the number of time steps that a node has to remain inactive before it can be wetted; for all of the results in this paper, that parameter was set to 5 time steps.

Third, every landlocked wet node is tagged as inactive. A landlocked wet node is not connected to any active elements, and thus does not receive contributions to either side of

the equation corresponding to that node. For some bathymetries, this criterion allows a node to remain inactive even if its total water depth is larger than the minimum wetting height. However, this criterion only applies to lone active nodes surrounded by inactive nodes; if there is more than one active node, and thus one or more active elements, then the region is allowed to remain active.

2.2. Model problems

The studies in this paper utilize two similar model problems. Both are linear sloping beaches with an open ocean boundary on the left-hand side, and both are forced by a tidal amplitude. We chose this bathymetry because: (1) it allows for a comparison with an analytical solution, as discussed in Section 3.1; and (2) it allows for a simple test case before moving forward to more complicated bathymetries, as discussed in Section 4.

The first model problem is similar to a test problem presented by Luettich and Westerink [1] in an earlier ADCIRC wetting-and-drying paper. The problem has the following parameters (unless stated otherwise): a linear slope, an undisturbed length of 20 kilometers, a bathymetric depth at the open ocean boundary of 5 meters, a grid spacing of 250 meters, a time step of 10 seconds, a forcing amplitude of 0.25 meters, a tidal period of 12 hours (43,200 seconds), a duration of 4 tidal periods, a *cftau* value of 0.001 and a G value of 0.001 sec^{-1} (both defined in Section 3.3), a H_{min} value of 0.01 meters, and a U_{min} value of 0.01 meters per second. We will refer to this as Model Problem 1.

The second model problem creates a situation where waves can wet and dry a larger number of nodes on the beach. This problem is deeper but shorter, and it allows wave run-up to cover more of the beach. This problem has the following parameters (unless stated otherwise): a linear slope, an undisturbed length of 18 kilometers, a bathymetric depth at the open ocean boundary of 6 meters, a grid spacing of 250 meters, a time step of 10 seconds, a forcing amplitude of 1.0 meter, a tidal period of 12 hours (43,200 sec), a duration of 4 tidal periods, a *cftau* value of 0.001 and a G value of 0.001 sec^{-1} (both defined in Section 3.3), a H_{min} value of 0.01 meters, and a U_{min} value of 0.01 meters per second. We will refer to this as Model Problem 2.

2.3. Error computations

Our sensitivity studies utilize a comparison between our numerical results and the analytical solution described in Section 3.1. This comparison is calculated through an examination of the position of the wet/dry interface over the fourth tidal period (because the model is spun up from a cold start for the first three periods). After every 10 minute interval in that fourth period, we calculate the difference between the position of the interface given by the numerical results and the position of the interface given by the analytical solution. These differences are then averaged. If the numerical results successfully approximate the analytical solution, then the average difference should be zero. However, spatial discretization often prevents a perfect match between numerical and analytical, so we are satisfied if the average difference is less than the grid spacing of 250 meters.

Our studies also utilize a computation of mass balance error. This is a cumulative mass balance error over the entire simulation. It is calculated using a finite volume approach, where we compute the difference between the global accumulation and the global mass flux, as represented by the primitive continuity equation. Recently, several papers [8,9] have advocated computing mass balance from finite element residuals in order to be

consistent with the numerical discretization. However, we have shown (Kolar et al. [13]) the finite volume approach to be a good surrogate variable for accuracy and phasing errors; that is, small mass balance errors (as computed with finite volume) correlate with small constituent errors. Hence our reason for using the finite volume approach herein.

3. NUMERICAL EXPERIMENTS

In this section, we discuss the results of several tests involving the wetting and drying algorithm. First, we compare the numerical results with an analytical solution. Second, we examine the algorithm's effect on temporal stability. Third, we conduct parameter sensitivity studies for bottom friction and the G numerical parameter. Fourth, we conduct parameter sensitivity studies for the wetting and drying parameters H_{min} and U_{min}. Fifth, we examine the effect of spatial resolution on the performance of the algorithm.

3.1. Comparison with an analytical solution

The classic analytical solution for wave run-up on a sloping beach was first expressed by Carrier and Greenspan [10] and later revisited by Johns [11] and Siden and Lynch [12]. The solution is quite restrictive; it describes the behavior of a frictionless wave on a linearly-sloped beach. The one-dimensional wetting-and-drying ADCIRC model incorporates bottom friction and can be applied to complex bathymetries. However, it is important to verify its performance against an analytical solution in this simple test case.

The full equations for the analytic solution are given in the latter two references. We will reproduce the important ones here. The equations for the velocity, horizontal position, and elevation of the shoreline are given by:

$$u = \frac{\partial \xi}{\partial t} = -u\frac{\partial u}{\partial t} - \frac{2A\pi}{T}\left(1 + \frac{\partial u}{\partial t}\right)\sin\left(\frac{2\pi}{T}(t+u)\right), \tag{2}$$

$$\xi = -\frac{1}{2}u^2 + A\cos\left(\frac{2\pi}{T}(t+u)\right), \tag{3}$$

and

$$\zeta = \xi \tag{4}$$

where u is the scaled velocity, ξ is the scaled horizontal displacement, A is the scaled amplitude, T is the scaled period, t is the scaled time, and ζ is the scaled free surface elevation from the mean. Note that Equation 4 holds true because the scaling changes the slope to 45 degrees. We solve for u in Equation 2 by using an iterative technique, a finite difference approximation of the $\partial u/\partial t$ terms, and the knowledge that the velocity of the shoreline at maximum inundation is zero. Once the shoreline information is calculated, then the velocity and elevation at interior points can be calculated using the following equations:

$$u = -\frac{4AJ_1\left(\frac{4\pi\sqrt{\zeta - x}}{T}\right)}{\alpha}\sin\left(\frac{2\pi}{T}(t+u)\right), \tag{5}$$

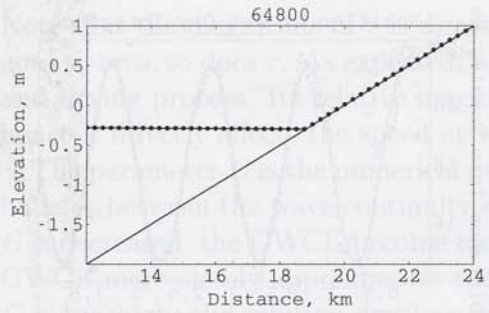

Figure 1. The numerical results (black dots) and the analytical solution (solid line) halfway through the second tidal cycle. Note that the number at the top of the figure is the time in seconds.

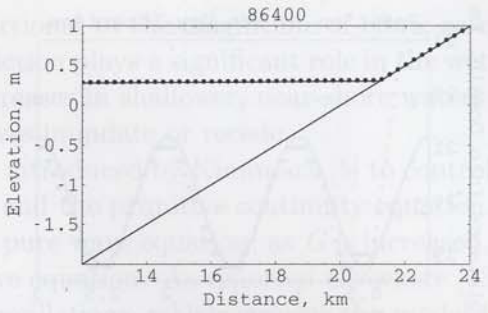

Figure 2. The numerical results (black dots) and the analytical solution (solid line) at the end of the second tidal cycle. Note that the number at the top of the figure is the time in seconds.

and

$$\zeta = -\frac{1}{2}u^2 + AJ_0\left(\frac{4\pi\sqrt{\zeta - x}}{T}\right)\cos\left(\frac{2\pi}{T}(t+u)\right), \tag{6}$$

where J_0 and J_1 are Bessel functions and x is scaled horizontal position. Equation 5 and Equation 6 must also be solved iteratively. Note that the ADCIRC boundary forcing was adjusted to match the cosine forcing of the analytical solution.

We attempted to match our numerical results with the analytical solution by using Model Problem 1. Figure 1 and Figure 2 show the analytical solution and numerical results at two points in the second tidal cycle. (Without a ramp function to smooth the transition from a cold start, the numerical solution experiences some start-up noise during the first tidal cycle.) Note that the numerical results shows good agreement with the analytical solution and that there is no friction-induced lag at the shoreline. We believe the good agreement is due to our relatively small value of *cftau*, so that the bottom friction does not dominate the momentum balance.

Figure 3 shows the position of the shoreline over the first three tidal periods. (This is similar to Figures 2 and 3 in Johns [11].) After the numerical results fight through the noise of the first tidal period, they show very good agreement with the analytical solution. There is some visible lag during the wetting phase, which raises the question of whether we need to relax our wetting criterion. That question will be addressed in a parameter study in Section 3.4; for now, we believe the information in these figures shows that the ADCIRC model can provide accurate results for this simple test case.

3.2. Heuristic stability

Stability was measured by determining the maximum time step (within 5 seconds) at which the model still provided valid results. However, it is difficult to measure the impact of the wetting and drying algorithm on stability because our model problems cannot be

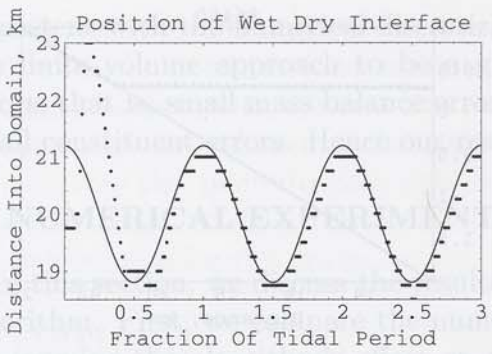

Figure 3. The position of the shoreline, as given by the numerical results (black dots) and the analytical solution (solid line) for the first three tidal periods.

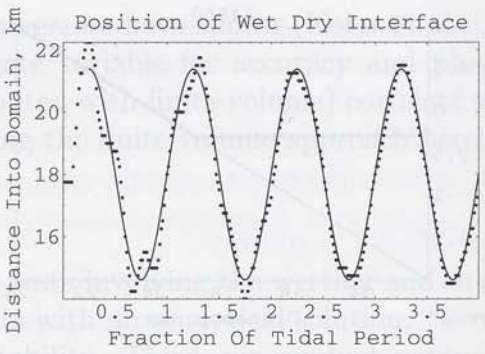

Figure 4. The position of the shoreline, as given by the numerical results (black dots) and the analytical solution (solid line) for the first four tidal periods.

run with the original fixed-boundary ADCIRC model. In order to prevent instabilities during the ebb phase when nodes should dry but cannot, we altered our model problems so that they could be run with the original model.

For Model Problem 1, we shortened the domain to 16 kilometers so that there is a bathymetry of 1 meter at the land boundary. This prevents the 0.25 meter forcing amplitude from trying to dry out nodes on the beach. All of the other parameters, including the slope, remained the same. Under these conditions, the original ADCIRC model provided a maximum stable time step of 60 seconds. The wetting and drying model, when applied to the unaltered Model Problem 1, provided a maximum stable time step of 55 seconds. This is a decrease of 8.3 percent.

For the more nonlinear Model Problem 2, we shortened the domain to 12 kilometers so that there is a bathymetry of 2 meters at the land boundary. This prevents the 1 meter forcing amplitude from trying to dry out nodes on the beach. All of the other parameters, including the slope, remained the same. The original ADCIRC model provided a maximum stable time step of 50 seconds. The wetting and drying model, when applied to the unaltered Model Problem 2, provided a maximum stable time step of 15 seconds. This is a decrease of 70 percent.

Note that, for both problems, mass balance errors were a order of magnitude greater for the wetting and drying model. These errors were concentrated on the beach where nodes are turned on and off.

3.3. Parameter sensitivity—*cftau* and *G*

Two important parameters in the ADCIRC model are *cftau* and G, the former being a physical parameter and the latter being purely numerical. The parameter *cftau* controls bottom friction in the model. It is used as a coefficient in the calculation of the equivalent linear bottom friction coefficient, τ, in the momentum equation for each node i:

$$\tau_i = cftau\left(\frac{|u_i|}{H_i}\right), \tag{7}$$

Note that the magnitude of τ is directly proportional to the magnitude of *cftau*; as *cftau* goes to zero, so does τ. As expected, bottom friction plays a significant role in the wetting and drying process. Its relative magnitude increases in shallower, near-shore waters and hence it directly affects the speed at which waves inundate or recede.

The parameter G is the numerical parameter introduced by Kinnmark [5] to control the balance between the wave continuity equation and the primitive continuity equation. As G is decreased, the GWCE become more like a pure wave equation; as G is increased, the GWCE more closely approximates the primitive equation. As reported elsewhere [13], if G is too high, the solution develops spurious oscillations, which prevent the model from capturing the behavior of the waves.

Because these two parameters are related in their effects on the model's behavior, it is important to examine them in tandem. Kolar et al [13] determined an optimal range of G/τ to be on the order of 1 to 10. However, that study examined the effects of these parameters on barotropic tides without wetting and drying. Herein, we examine their effects on wetting and drying by varying the parameters *cftau* and G from 0.000001 to 0.5 (always in sec^{-1} for G; *cftau* is dimensionless), creating a matrix of *cftau*-G combinations. For each combination, we compared the behavior of the model with the analytical solution described above, and we examined the model's mass balance properties. The tests in this section use Model Problem 2.

The comparison with the analytical solution was performed by averaging the differences between the numerical results and the analytical solution over the fourth tidal cycle, as discussed above in Section 2.3. By plotting these averages for each combination in the matrix, we developed a three-dimensional surface that cannot be meaningfully reproduced in this space. However, we can share some observations from this surface. First, the model is unstable in almost one fourth of the matrix, in the region where both *cftau* and G approach 0.000001. It is stable, however, in the regions where only one of these parameters approaches this minimum value. Second, the model is significantly more sensitive to variations in *cftau*. The variations with regard to G are not nearly so pronounced.

Third, in general, the average differences between the numerical results and the analytical solution decrease as *cftau* is decreased. This trend is intuitive, considering the analytical solution is frictionless. A slice of the matrix where *cftau* is held constant at a value of 0.000001 and G is varied would show average differences on the magnitude of three times the grid spacing of 250 meters.

Interestingly, the best agreement between the numerical results and the analytical solution occurs with a combination such as $cftau = 0.0001$ and $G = 0.01\ sec^{-1}$, which provides an average difference of 211 meters, or less than one grid spacing. Figure 4 shows the position of the wet/dry interface over time for a simulation using this combination. The numerical results experience some start-up noise during the first two tidal cycles, but then they show good agreement with the numerical solution during the fourth tidal cycle. We will use this combination of *cftau* and G in Section 3.4, where we are explicitly trying to match the analytical solution. However, it should be remembered that the analytical solution does not include bottom friction, so it will not be accurate for all situations. In general, the values of *cftau* and G should be determined based on the bottom friction requirements of the particular simulation.

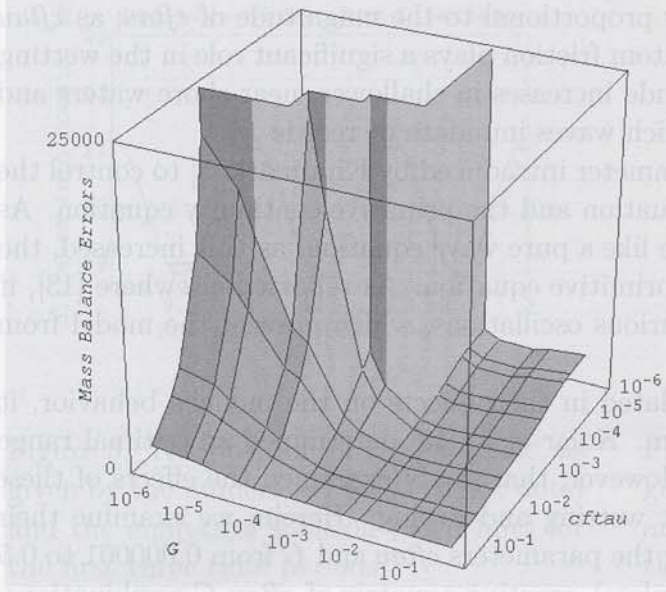

Figure 5. Mass balance errors for 144 combinations of *cftau* and G. The errors in the region at the front of the graph are on the order of 1,000 to 2,000 square meters.

The examination of the model's mass balance properties was performed in the same manner, by creating a matrix of *cftau*-G combinations. The mass balance error was calculated using the finite volume approach, described in Section 2.3. Using these average mass balance errors, we created another three-dimensional surface, this time shown in Figure 5. The model is unstable for the same region of combinations, where both *cftau* and G approach 0.000001. However, if G remains relatively large, then *cftau* can be decreased without significant penalty. For example, a typical range of *cftau* from 10^{-3} to 10^{-5} shows: (1) mass balance errors on the order of 2,000 square meters, or approximately 3.7 percent of the total undisturbed water area; and (2) when G is decreased to its minimum stable value, ratios of G/τ are in the range of 1 to 10 (optimum range reported by Kolar et al. [13] in their fixed-boundary barotropic studies). Note that values of *cftau* larger than 10^{-3} do show good mass balance, but they produce unrealistically damped simulations.

3.4. Parameter sensitivity - *Hmin* and *Umin*

Another pair of important numerical parameters is *Hmin* and *Umin*, described above in Section 2.1. Both parameters affect the ability of the algorithm to wet or dry nodes. The parameter *Hmin* controls the drying phase, and the parameter *Umin* controls the wetting phase. For example, a large value for *Hmin* would allow nodes to dry while still holding a significant amount of water, causing nodes to dry much faster than they should. Similar problems would be experienced if the value for *Hmin* is too small or if the value of *Umin* is at either extreme. Thus, it is important to consider the effects of the two parameters in tandem.

We accomplished this consideration by using the same technique as for *cftau* and G. We examined the effects of *Hmin* and *Umin* by varying each parameter from 0.0001 to 0.5

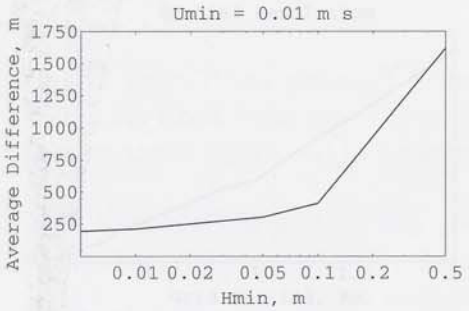

Figure 6. The average difference (in meters) between the numerical results and the analytical solution in their calculation of the position of the shoreline over the fourth tidal cycle. (See Section 2.3.)

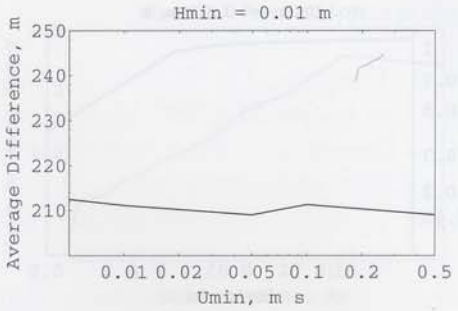

Figure 7. The average difference (in meters) between the numerical results and the analytical solution in their calculation of the position of the shoreline over the fourth tidal cycle. (See Section 2.3.)

(meters for H_{min}; meters per second for U_{min}), creating a matrix of H_{min}-U_{min} combinations. For these runs, we used $cftau = 0.0001$ and $G = 0.01\ sec^{-1}$ which the previous study found to produce meaningful solutions. We also used Model Problem 2. For each combination of H_{min} and U_{min}, we compared the behavior of the model with the analytical solution and we examined the model's mass balance properties.

The comparison with the analytical solution was performed by using the same technique as above, where we built a matrix of average differences between the numerical results and the analytical solution. We offer the following observations. First, the model does not go unstable anywhere in the range from 0.0001 to 0.5. In fact, we were able to successfully decrease H_{min} to 10^{-10} meters; the model behaves similarly for all values of H_{min} less than 0.01 meters, as shown in Figure 6. However, increasing H_{min} beyond the upper limit of this range does cause instabilities, especially for unrealistic values such as 10 meters.

Second, the parameter U_{min} has no significant effect on the behavior of the model for the conditions of this problem. Figure 7 shows a slice where H_{min} has a constant value of 0.01 meters and U_{min} is varied. In this graph, there is no noticeable change between the average differences for the extreme values of $U_{min} = 0.0001$ meters per second and $U_{min} = 0.5$ meters per second. Similar behavior was observed when H_{min} was held to other constant values, i.e., results are insensitive to the parameter U_{min} for this test problem.

The examination of the model's mass balance properties was performed in the same manner as described in Section 2.3. The mass balance error was calculated by computing the difference between the global accumulation and the global mass flux. A three-dimensional surface of average mass balance errors over four tidal cycles revealed the following. First, again, the model does not experience instabilities for any combination of H_{min} and U_{min} within the range from 0.0001 to 0.5. Second, the wetting criterion U_{min} does not have an effect on mass balance. Third, the average mass balance errors decrease as H_{min} is increased. Figure 8 shows that the errors decrease from a steady 1100 square meters when H_{min} is less than 0.01 to about 400 square meters when $H_{min} = 0.5$. However,

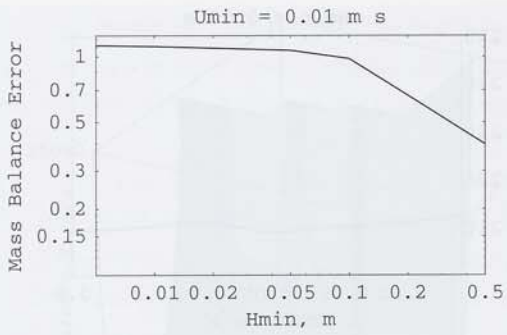

Figure 8. Mass balance errors for a range of H_{min} values. The horizontal axis is H_{min} in log scale. The vertical axis is mass balance errors (10^3 square meters) in log scale.

this decrease is at the expense of accuracy, as discussed above and shown in Figure 6. For such a large value of H_{min}, the numerical results are unable to match the analytical solution.

Thus, results indicate an optimal value for these two parameters are H_{min} and U_{min} is around 0.01. There does not appear to be a lower limit for either parameter; however, nothing is gained by decreasing either parameter to the limits of machine precision. We will continue to use values of 0.01 for both parameters.

3.5. Spatial resolution

Spatial resolution also plays a significant role in the simulation of wetting and drying, because it controls the model's ability to follow the position of the shoreline as it inundates and recedes. Using Model Problem 2, we varied the spatial resolution from a minimum of 100 meters to a maximum of 2000 meters. For each grid spacing, we compared the behavior of the model with the analytical solution and we examined the model's mass balance properties.

Figure 9 shows the average difference between the numerical results and the analytical solution for the various spatial resolutions. Note that all of the simulations were run with a time step of 10 seconds except for those with spatial resolutions of 100 meters and 120 meters, which were run with a time step of 1 second in order to maintain stability. The graph shows a sublinear convergence rate as the grid spacing is decreased.

Figure 10 shows the mass balance errors for the various spatial resolutions. This graph supports the use of the finite volume approach as a predictor of model behavior because, as the grid spacing is decreased, the mass balance errors also decrease.

4. CONCLUSIONS AND FUTURE WORK

Based on the studies in this paper, we offer the following conclusions:

- ADCIRC's wetting and drying algorithm can simulate wave run-up on a frictionless beach, even one tidal period after a cold start.
- The algorithm imposes stability restrictions, which can be severe in nonlinear appli-

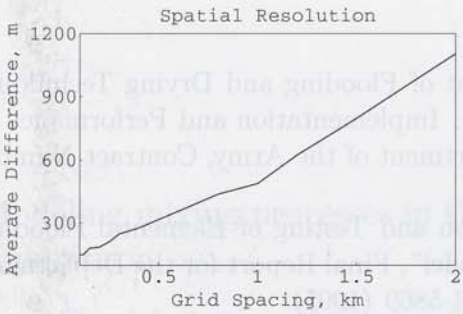

Figure 9. The average difference between the numerical results and the analytical solution. (See Section 2.3.)

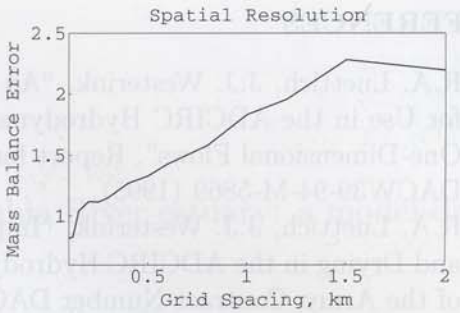

Figure 10. Mass balance errors (10^3 square meters) for a range of spatial resolutions. (See Section 2.3).

cations. Our Model Problem 2 experienced a 70 percent reduction in the maximum stable time step, as compared to a fixed-boundary simulation.

- The numerical parameter G must remain relatively large (i.e., greater than 0.001 sec^{-1}), especially for typical values of *cftau* in the range from 0.001 to 0.00001. However, combinations of *cftau* and G in that range show reasonable mass balance errors and values of G/τ in the same range as for non-wetting/drying barotropic applications.
- The minimum wetness height H_{min} shows acceptable behavior for all values less than or equal to 0.01 meters.
- The minimum wetting velocity U_{min} has no significant effect on the behavior of the model under these conditions.
- Accuracy and mass balance improve as the spatial resolution is refined. However, a stability restriction prevents simulations with grid spacings of 100 meters and 120 meters from being run with the same time step of 10 seconds.

Future work will focus on other domains, such as an idealized grid with a quadratic bathymetry and a realistic domain based on a slice of the Beaufort Inlet in North Carolina, and alternative error measures, such as least squares. Through a better understanding of the behavior of ADCIRC's wetting and drying algorithm, we hope to offer a guideline for spatial resolution in near-shore areas.

ACKNOWLEDGMENTS

Financial support for this research was provided, in part, by the National Science Foundation under the contract EEC-9912319, the Department of Defense under the contract ONR N00014-02-1-0651, and the University of Oklahoma. Any opinions, findings, and conclusions or recommendations expressed in this material are those of the authors and do not necessarily reflect those of the funding agencies.

REFERENCES

1. R.A. Luettich, J.J. Westerink, "An Assessment of Flooding and Drying Techniques for Use in the ADCIRC Hydrodynamic Model: Implementation and Performance in One-Dimensional Flows", Report for the Department of the Army, Contract Number DACW39-94-M-5869 (1995).
2. R.A. Luettich, J.J. Westerink, "Implementation and Testing of Elemental Flooding and Drying in the ADCIRC Hydrodynamic Model", Final Report for the Department of the Army, Contract Number DACW39-94-M-5869 (1995).
3. R.L. Kolar, W.G. Gray, J.J. Westerink, R.A. Luettich, "Shallow water modeling in spherical coordinates: equation formulation, numerical implementation and application", *Journal of Hydraulic Research*, **32(1)**, 3-24 (1994).
4. D.R. Lynch, W.G. Gray, "A wave equation model for finite element tidal computations", *Computers and Fluids*, **7(3)**, 207-228 (1979).
5. I.P.E. Kinnmark, "The shallow water wave equations: formulations, analysis and application", in *Lecture Notes in Engineering*, C.A. Brebbia, S.A. Orsszag (eds), Springer-Verlag, Berlin, **15**, 187 (1986).
6. R.A. Luettich, J.J. Westerink, N.W. Scheffner, "ADCIRC: an advanced three-dimensional circulation model for shelves, coasts and estuaries. Report 1: theory and methodology of ADCIRC-2DDI and ADCIRC-3DL", Technical Report DRP-92-6, Department of the Army, USACE, Washington, DC (1992).
7. J.J. Westerink, R.A. Luettich, C.A. Blain, N.W. Scheffner. "ADCIRC: an advanced three-dimensional circulation model for shelves, coasts and estuaries. Report 2: Users Manual for ADCIRC-2DDI", Department of the Army, USA (1994).
8. T.J.R. Hughes, G. Engel, L. Mazzei, M.G. Larson, "The continuous Galerkin method is locally conservative", *Journal of Computational Physics*, **163(2)**, 467-488 (2000).
9. R.C. Berger, S.E. Howington, "Discrete Fluxes and Mass Balance in Finite Elements", *Journal of Hydraulic Engineering*, **128(1)**, 87-92 (2002).
10. G.F. Carrier, H.P. Greenspan, "Water waves of finite amplitude on a sloping beach", *Journal of Fluid Mechanics*, **4**, 97-109 (1958).
11. B. Johns, "Numerical Integration of the Shallow Water Equations over a Sloping Shelf", *International Journal for Numerical Methods in Fluids*, **2**, 253-261 (1982).
12. G.L.D. Siden, D.R. Lynch, "Wave Equation Hydrodynamics on Deforming Elements", *International Journal for Numerical Methods in Fluids*, **8**, 1071-1093 (1988).
13. R.L. Kolar, J.J. Westerink, M.E. Cantekin, C.A. Blain, "Aspects of Nonlinear Simulations using Shallow-Water Models based on the Wave Continuity Equation", *Computers and Fluids*, **23**, 523-538 (1994).